Ocean Engineering 240 (2021) 109958

Contents lists available at ScienceDirect

Ocean Engineering

journal homepage: www.elsevier.com/locate/oceaneng

A Recurrent-Cascade-Neural network- nonlinear autoregressive networks with exogenous inputs (NARX) approach for long-term time-series prediction of wave height based on wave characteristics measurements

Yehia Miky [a,b,*], Mosbeh R. Kaloop [c], Mohamed T. Elnabwy [d], Ahmad Baik [a], Ahmed Alshouny [a,e]

[a] Department of Geomatics, Faculty of Architecture and Planning, King AbdulAziz University, Jeddah, Saudi Arabia
[b] Civil Engineering Department, Faculty of Engineering, Aswan University, Aswan, Egypt
[c] Public Works Engineering Department, Mansoura University, Mansoura, Egypt
[d] Coastal Research Institute, National Water Research Center, Alexandria, Egypt
[e] Survey Research Institute, National Water Research Center, Giza, Egypt

A R T I C L E I N F O

Keywords:
Significant wave height
Average wave period
NARX
Wavelet
Neural networks

A B S T R A C T

To overcome the data limitations of wave and environmental characteristics for estimating the significant wave height (Hs), this study investigates the use of an available dataset for wave characteristics to predict a long-term period of Hs for the Red Sea. A novel soft-computing approach is designed for the time-series prediction of Hs using the time delay of average wave period and Hs measurements. Buoy station of Jeddah, Saudi Arabia, datasets for 2009 and 2010 are used for designing and validating the proposed model. The time-series identification system of nonlinear autoregressive networks with exogenous inputs (NARX) and recurrent neural network (RNN) with cascade input variables based on neural network solutions were integrated through a sequential system to develop the new approach RNNARX. The RNNARX was compared with the conventional RNN, NARX neural network (NNARX), and previous studies' results to verify its robustness. The proposed model was evaluated to predict hourly and daily Hs. The results showed that the proposed model achieves good performance for long-term prediction of Hs. The sequential system improved the performance of RNN and NNARX models for the time-series prediction of Hs. The comparison results showed that RNNARX performance is suitable for the Hs prediction of the study region. The model performances in terms of coefficient determination and root mean square error were 0.90 and 0.149 m, respectively, with a prediction error of 2.95% for four days lead times.

1. Introduction

Onshore and offshore engineering applications, as well as marine and coastal activities, require accurate prediction for the significant wave heights, or simply wave height (Hs), of seas or oceans worldwide. Many researchers designed and evaluated different prediction models for Hs in different regions (Emmanouil et al., 2020; Kumar et al., 2017, 2018; Ti et al., 2018; Zubier and Eyouni, 2020). The common prediction models employed wave and environmental characteristics for estimating Hs (Table 1). Numerical and physical models can be used to estimate the wave characteristics (Ardhuin and Herbers, 2005; Blackmar et al., 2014; Chen et al., 2016). The changing wind is the major influence on wave generation and height (WMO, 1998). However, the processing wave generation is complex, which compromises many forces and parameters (see WMO (1998) for more details). For time-consuming, soft-computing methods, as a numerical solution, have found good tools for predicting Hs. Table 1 presents some of the most recent (2012–2020) approaches designed and applied for Hs prediction.

From Table 1 and previous studies (Etemad-Shahidi and Mahjoobi, 2009; James et al., 2018; Mahjoobi and Mosabbeb, 2009; Akhil and Deka, 2017; Peres et al., 2015), it can be seen that the most proposed models achieve good performance on short-term time leads. The long-term time-series prediction models are limited to Hs prediction, and the best fitting (in terms of R^2) for 3-days' lead times is 0.593. Additionally, the table shows that the time delay of Hs and wind speed can be used for Hs prediction. This is due to the high correlation between wind speed and Hs. Moreover, Table 1 shows that the conventional and hybrid soft-computing methods are applied and can be used to estimate

* Corresponding author. Department of Geomatics, Faculty of Architecture and Planning, King AbdulAziz University, Jeddah, Saudi Arabia.
E-mail addresses: yhhassan@kau.edu.sa (Y. Miky), mosbeh@mans.edu.eg (M.R. Kaloop), Mohamed_elnabwy@nwrc.gov.eg (M.T. Elnabwy), Abaik@kau.edu.sa (A. Baik), ametaowa@kau.edu.sa (A. Alshouny).

https://doi.org/10.1016/j.oceaneng.2021.109958
Received 15 February 2021; Received in revised form 21 September 2021; Accepted 1 October 2021
Available online 9 October 2021

Table 1
Summary of recent soft-computing models for Hs prediction.

Model	Input variable	Region('s)	R^2	Ref
Wavelet-ANN	Hs	Canada, India	0.930@ 3 h	Prahlada and Deka (2015)
LSTM	WD, WS, Hs	Korea, Brazil, UK, Spain, USA	0.593@ 3 d	Fan et al. (2020)
WPSO-ELM	GS, AP, Ta, Hs	USA	0.577@ 36 h	(Kaloop et al., 2020a)
ANN	D, GS, P, Ta, Tw, AP, Hs	Gulf of Mexico	0.563@ 24 h	Mafi and Amirinia (2017)
Ens-ELM	wave and atmospheric conditions	Gulf of Mexico, Korea, Brazil	0.920@ 1 h	Kumar et al. (2018)
MLR-CWLS	Wave conditions, Tw, Hs	Australia	0.950@ 0.5 h	Ali et al. (2020)
DBN-IF	WS, GS, AP, Ta, Hs	Korea, USA	0.566@ 24 h	Li and Liu (2020)
ELM	WS, Hs	Arabian Gulf	0.820@ 0.5 h	Shamshirband et al. (2020)
M5T	AP, WS, Tw, P	USA	0.831 @ 0 h	Kaloop et al. (2020b)
ANN & ANFIS	Hs	Arabian Sea	0.903@ 24 h	Vimala et al. (2012)
SVM-FFA	WS, WD, Ta, Tw	USA	0.979@ 1 h	Roy et al. (2016)
NARX	Hs	Caspian Sea	0.78@ 24 h	Sadeghifar et al. (2017)
ANN-deep learning	P, WS, GS	Sea of Japan	0.90@ 12 h	Tom et al. (2019)

ANN: Artificial Neural Networks; LSTM: Long Short-Term Memory network; WPSO-ELM: Wavelet-Particle Swarm Optimization-Extreme Learning Machine; Ens-ELM: Ensemble of Extreme Learning Machine; MLR-CWLS: Multiple Linear Regression-Covariance-Weighted Least Squares algorithm; DBN-IF: Dynamic Bayesian Network-Information Flow; M5T: M5 regression tree; ANFIS: Adaptive Network-based Fuzzy Inference System; SVM-FFA: Support Vector Machine-Firefly Algorithm; NARX: nonlinear autoregressive networks with exogenous. R^2 is the coefficient of determination.
WD, WS, GS represent the wind direction, speed, and gust wind speed, respectively. D is the water depth. Ta and Tw are the air and water temperature, respectively. P is the water pressure. AP is the hourly average wave period. Wave and atmospheric conditions are all variables of wave and atmospheric that available on NOAA's website.

appropriate accuracy in predicting Hs for up to 3-days' lead times in maximum. This study improves the accuracy of Hs prediction for more than 3-days' lead times using a novel design of a hybrid soft-computing method.

The main advantage of soft-computing methods is the impact of finding nonlinear solutions between inputs and outputs for modeling (Roy et al., 2016). The common method used for Hs prediction is artificial neural networks (ANN) and integration with other methods (Table 1). Shallow and deep ANN models have been developed for Hs prediction (Kumar et al., 2017; Tom et al., 2019). Sequential ANN was applied to predict the daily wave heights (Kumar et al., 2017). It can be considered as an in-between solution of shallow and deep soft-computing algorithms, which decreases the complicity of deep learning solutions. In this study, a hybrid recurrent and cascade ANN with multiple hidden layers of nonlinear autoregressive networks with exogenous inputs (NNARX) is proposed as a sequential ANN-NARX solution for Hs prediction.

Recurrent ANN (RNN) employs internal memories of ANN to express temporal dynamic behavior, making it suitable for modeling complex performances of signals (Pirhooshyaran and Snyder, 2020). Furthermore, it was applied through NARX for predicting hourly Hs, and the correlation between the observed and predicted Hs is 0.87 for 12 h lead times (Mandal and Prabaharan, 2006). Additionally, it was applied to predict floods, and the results showed that the performance is high (Le et al., 2019). The recurrent time step affects the time-consuming of the model processing. Thus, feedforward ANN was applied to estimate the

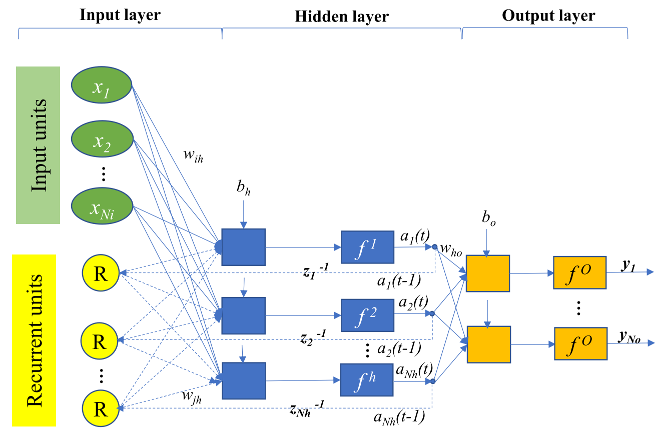

Fig. 1. Elman RNN diagram.

Hs, but the data volume and the number of ANN hidden layers are important factors for improving the model's accuracy (Gopinath and Dwarakish, 2016; Paplińska-Swerpel and Paszke, 2006; Shamshirband et al., 2020). However, cascade ANN was applied to improve the feedforward techniques by increasing the complexity of ANN architecture (Kanan and Faez, 2004). The cascade ANN performance is significant for Hs prediction, up to 24 h, and it was integrated with backward-propagation and gradient descent (Kanan and Faez, 2004; Deo and Naidu, 1998). The NARX is one of the powerful feedforward or RNN techniques for nonlinear dynamic systems using time-series identification approaches (Yetkin and Kim, 2019; Yetkin et al., 2017). NARX has been applied alone and integrated with other methods to improve the forecasting models. For instance, the autoregressive (AR) was integrated with ANN to improve the rainfall predicting model in Southwestern Colombia (Canchala et al., 2020). Additionally, AR was integrated with an empirical mode decomposition to predict nonstationary waves, which improve the Hs prediction up to 6 h ($R^2 = 0.94$) (Duan and Huang, 2016). NARX and RNN were integrated to improve the streamflow estimation, and the results provided that the combination reduced the uncertainty of discharges by 50% (Tian et al., 2018). Furthermore, the hybrid RNN-NARX improved the prediction of Chaotic time-series (Ardalani-Farsa and Zolfaghari, 2010). The coastal Hs prediction was determined by integrating NARX and RNN, and the results showed that the performance of the proposed model is high up to 24 h lead times ($R^2 = 0.78$) (Sadeghifar et al., 2017).

Therefore, this study designs a new model that can be used to predict Hs for more than three days ahead. Thus, the RNN, cascade ANN, and NNARX are integrated to design the proposed model RNNARX. The data of two years for wave characteristics (Hs and AP) are used to design and validate the proposed model. The proposed model is designed and applied for predicting coastal Hs. The data from a buoy (station No. 2320, on the NOAA's website), in the Red Sea, off Jeddah, Saudi Arabia, are used. There are no long-term studies on Hs prediction in this region since the data are non-available and limited. Thus, the output of this research may help in long-term time-series Hs prediction of this region.

2. Methods

2.1. Cascade and recurrent artificial neural networks

The principal theory and algorithm of ANN can be found in (Mathworks, 2016; Schmidhuber, 1992; Warsito et al., 2018). The conventional ANN consists of three layers: input, hidden, and output layers. The connections between these layers are weights between the layers. In this study, the cascade-forward ANN (CFNN) and RNN are implemented as a part of ANN. The CFNN model for time-series prediction of $\boldsymbol{y(t)}$ using $\boldsymbol{x(t)}$ variable inputs can be expressed as follows (Warsito et al., 2018):

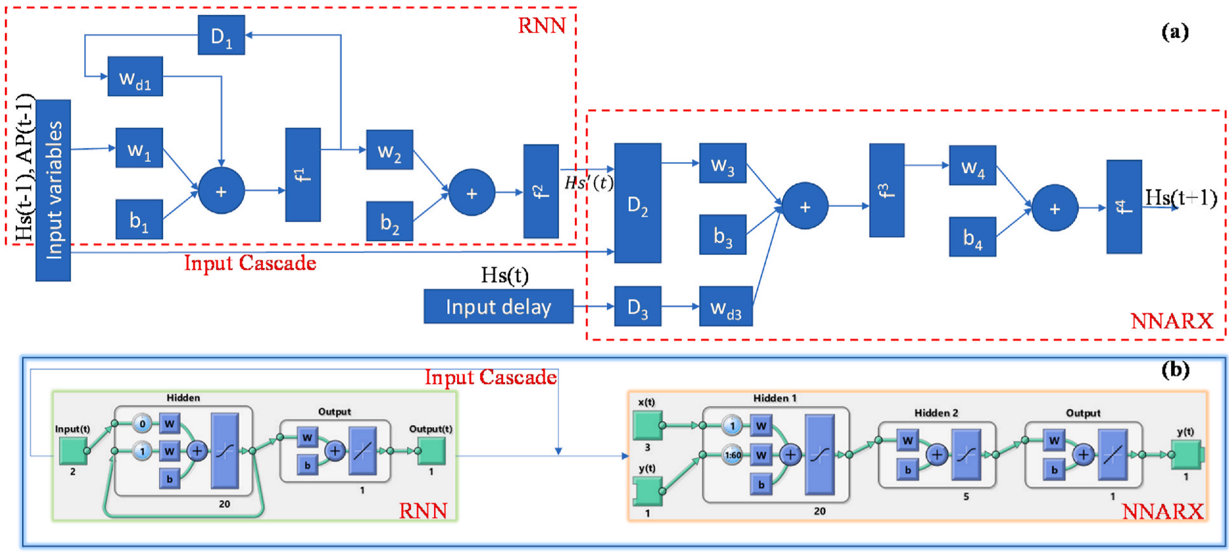

Fig. 2. Designed RNNARX model diagram, (a) overall model diagram and (b) Matlab diagram for 5 days prediction of Hs.

$$y(t) = \sum_{i=1}^{Ni} f^i w_i^i x_i + f^o\left(b_o + \sum_{j=1}^{Nh} w_j^o f^h\left(b_h + \sum_{i=1}^{Ni} w_{ji}^h x_i\right)\right), \quad (1)$$

where, f^i is the activation function from the input to output layers; f^o and f^h are the functions of output and hidden layers, respectively. ***w*** represents the weight connection between layers, and b_o and b_h are the biases of outputs and hidden units, respectively. *Ni* and *Nh* are the numbers of inputs and hidden neurons, respectively; $i = 1, 2, \ldots, Ni$ and $j = 1, 2, \ldots, Nh$.

The Elman network is applied in this study for RNN (Ardalani-Farsa and Zolfaghari, 2010; Elman, 1990). Fig. 1 presents the Elman RNN diagram. The Elman network contains a recurrent layer besides ANN layers. The RNN model for time-series prediction of ***y(t)*** using ***x(t)*** variable inputs can be expressed as follows (Ardalani-Farsa and Zolfaghari, 2010):

$$y(t) = f^o\left(\sum_{o=1}^{No} b_o + \sum_{h=1}^{Nh} w_{ho} f^h\left(b_h + \sum_{i=0}^{Ni} w_{ih} x_i + \sum_{j=0}^{Nh} w_{jh} z_h^{-1}\right)\right), \quad (2)$$

where, w_{ho}, w_{ih}, w_{jh} are the weight of the connections between the hidden and output layers, between the input and hidden layers, and between the recurrent and hidden layers, respectively. *No* is the number of output layers, $o = 1,2, \ldots No$, and $j,h = 1, 2, \ldots, Nh$. z_h is the outputs of the hidden nodes (*i.e.*, $z_{Nh} = a_{Nh}(t)$, and $z_{Nh}^{-1} = a_{Nh}(t-1)$), (as presented in Fig. 1).

2.2. Nonlinear autoregressive networks with exogenous inputs (NARX) neural network

NARX neural network (NNARX) is one of the ANN types. Feedforward and recurrent NNARX are used for time-series prediction approaches (Ardalani-Farsa and Zolfaghari, 2010; Xie et al., 2009). The processing of the feedforward system is suitable for time-series

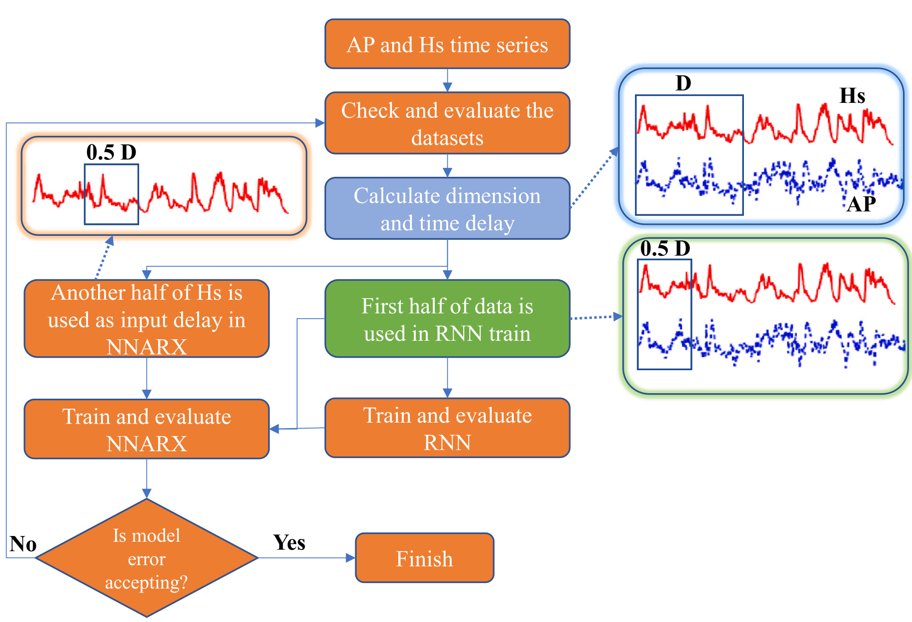

Fig. 3. Flowchart of data used and Hs prediction in RNNARX approach.

prediction (Xie et al., 2009). NNARX was found suitable for modeling nonlinear systems and time-series (Ardalani-Farsa and Zolfaghari, 2010; Yetkin and Kim, 2019). The NARX is a hybrid function of output system (AR) and external excitations (X), and it can be expressed as follows (Ardalani-Farsa and Zolfaghari, 2010):

$$y(t+1)=F\left(y(t),\ldots,\ y(t-d_y);x(t),\ldots,\ x(t-d_x)\right), \tag{3}$$

where, F is the NARX function, d_x and d_y are the input and output regressors, respectively.

In NNARX, the activation functions are used instead of NARX unknown function (Yetkin and Kim, 2019; Ardalani-Farsa and Zolfaghari, 2010). The general NNARX can be expressed as follows (Ardalani-Farsa and Zolfaghari, 2010):

$$y(t+1)=f^o\left(b_o+\sum_{h=1}^{Nh}w_{ho}f^h\left(b+\sum_{i=0}^{d_x}w_{ih}x(t-i)+\sum_{j=0}^{d_y}w_{jh}y(t-j)\right)\right), \tag{4}$$

The NNARX can be applied with single and multi-input variables. In this study, multi-input time-series of Hs and period are used to predict the time-series of Hs.

2.3. Proposed model

The proposed cascade-RNN-NNARX (RNNARX) is summarized and used for the long-term prediction of time-series of Hs in the Red Sea. The feedforward NNARX is also used. Fig. 2 shows the diagram of the RNNARX model and implemented Matlab diagram of the designed approach; in Fig. 2 a the w_i ($i=1,\ldots,4$) represents the connection weight of the input variables, $w_{d1} and w_{d3}$ are the weight connection of the Hs delay in RNN and NNARX, respectively, b_i ($i=1,\ldots,4$) denotes the biases, and $f^i(i=1,\ldots,4)$ denotes the activation functions. Appendices A1 and A2 present the algorithm and flowchart of the proposed model, respectively. The time-series of Hs and wave hourly average period (AP) at the current time were used to predict significant Hs in different lead times. The proposed model consists of RNN and NNARX with cascade input variables for improving the nonlinear system of Hs prediction. The predicted Hs from RNN is used with inputs Hs and AP and input delayed Hs to predict the Hs in different lead times. The designed model consists of one hidden layer in RNN and two hidden layers in NNARX (Fig. 2b). The designed numbers of hidden layers are presented in the result section. So, RNNARX with five hidden layers is designed and processed. For time-consuming, one delay ($D_1=1$) was used in RNN. In NNARX, the time head is used for the input delay of datasets, D2 = 1 for first the first half of input delay of Hs and AP and RNN output and D3 = half of lead time for second half of input delay of Hs. Fig. 3 presents the flowchart of data used and input delay in RNNARX for estimating the Hs. In other words, for improving the model results, the input variables are divided into two sections, the first is the half of datasets (Hs and AP), which are used in RNN, and another half of Hs are used as input delay in NNARX, as presented in Figs. 2 and 3. E.g., as presented in Fig. 2 b, for predicting 5 days' time head, the data of first 60 h is used in RNN and NNARX with D1 = D2 = 1, and the remaining data of Hs is used as input delay in NNARX with D3 = 60 h; moreover, the output Hs of RNN is used with D2 = 1 as a guidance layer. Both RNN and NNARX are trained by gradient descent with momentum and the Levenberg-Marquardt (LM) algorithm. Herein, different algorithms in Matlab were evaluated, and the results showed the LM algorithm outperformed other methods. The main advantage of the LM technique is that "it acts more like a gradient-descent and Gauss-newton methods when the parameters are far and close to their optimal values, respectively" (Gavin, 2020). The activation function of the hidden layer is the tan-sigmoid function ($f(x)=\frac{1}{1-e^{-2x}}-1$) and the linear activation function ($f(x)=x$) is used for input and output layers. For long-term prediction time-series of Hs, hourly time leads (1–12 h) and daily time heads (1–5 days) are examined.

Herein, previous Hs models overlooked the prediction of long-period of Hs. Hybrid RNN-NNARX, RNNARX, is developed in the current study to predict long period time series of Hs based on the high correlation between Hs and AP and from another side between current and delay Hs. This correlation means the prediction of Hs is not dependent on randomness observations. Herein, based on the theory of long short-term memory (LSTM) network and Chen and Chaudhari (2004) and Yuen et al. (2019) studies, divided input datasets and double steps networks can be used to improve the long-period prediction of time-series datasets. Replace the recurrent neural network and the forward subnetwork as conventional neural network systems by recurrent and double forward subnetworks with dividing data into both subnetworks through the cascade input is implemented. The LSTM and sequence networks systems were applied to overcome the vanishing gradient problem in recurrent and feedback neural networks (Chen and Chaudhari, 2004; Gers, 2001; Bolderman et al., 2021). In the current study, the correlation of the measurements is employed in predicting the long-period of Hs through using input-delay of Hs only in NNARX; this step is also used to overcome the vanishing gradient problem by decreasing the time lag in long-period prediction (Kolen and Kremer, 2001). Based on Fig. 3, the evaluation of the dataset is employed to detect any noises or errors; here the data used in this study were filtered from the data source (NDBC - Station 23020 Recent Data (noaa.gov)). The processing of data used in modeling is presented in Figs. 2 and 3. Based on the selected time delay (D), the processing of the proposed method is divided into two stages. In the first stage, the first half of the time delay is used in predicting Hs through the RNN approach. The recurrent ANN was found a powerful technique for complex nonlinear detection as presented in the introduction, so, one delay is used in RNN to reduce the time consuming and estimate the upcoming Hs ($Hs'(t)$) which has a high correlation with input delay Hs(t) of NNARX. Here, the output of RNN can be considered as a guidance layer (Bolderman et al., 2021). This step should improve the results, as presented in the results section, since the correlation between input variables is high. In addition, the current time series of Hs was found highly significant to predict Hs in different lead times, as presented in Table 1. In the second stage, the input delay Hs(t), which is the remaining half of D, and input cascade (Hs(t-1) and AP(t-1)) and RNN output ($Hs'(t)$) are used in NNARX for predicting Hs in D time head. Here, the input delay of Hs has decreased the long-time lags, which improve the model results in long period prediction. The trials of using RNN, NNARX, and developed models were studied, and evaluated in the result section. From the results of RNNARX, it can be concluded that the proposed model can be used to encounter the vanishing gradient problem in long-term prediction of Hs.

2.4. Model's performance evaluation

In this study, RNN, NNARX, and RNNARX are employed and evaluated. Different statistical indices are used to evaluate models' performance. R^2 is used to determine the correlation between the observed and predicted values. RMSE, mean absolute error (MAE), and maximum absolute error (XAE) are used to evaluate the model's errors. The percentage of RMSE (PE) is used to estimate the percentage of prediction errors for the models. These indices can be calculated as follows:

$$R^2=1-\frac{\sum(o_i-y_i)^2}{\sum(o_i-\overline{o})^2} \tag{5}$$

$$RMSE=\sqrt{n^{-1}\sum(o_i-y_i)^2} \tag{6}$$

$$MAE=n^{-1}\sum|o_i-y_i| \tag{7}$$

$$XAE=\max(|o_i-y_i|) \tag{8}$$

$$PE=\frac{RMSE}{o_{max}-o_{min}}\times 100 \tag{9}$$

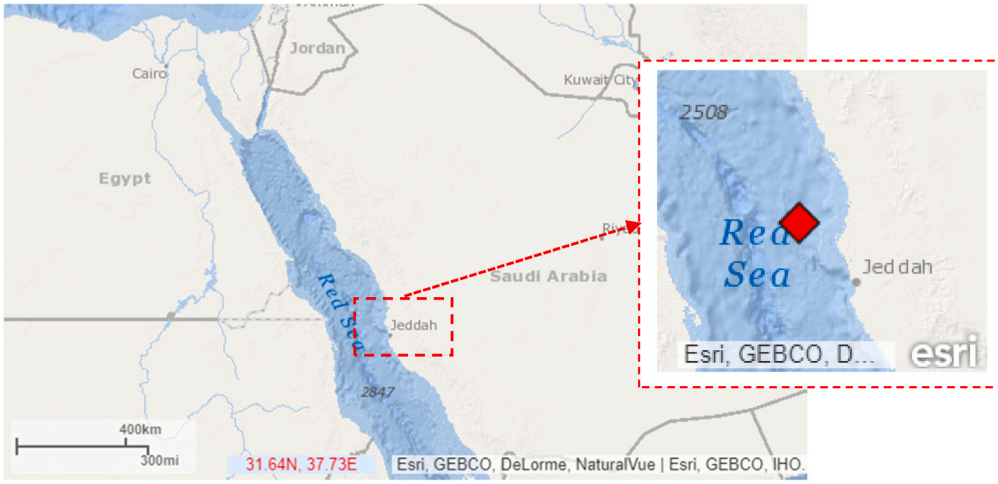

Fig. 4. Location of the Jeddah buoy station in the Red Sea (the figure source is NOAA website). (For interpretation of the references to colour in this figure legend, the reader is referred to the Web version of this article.)

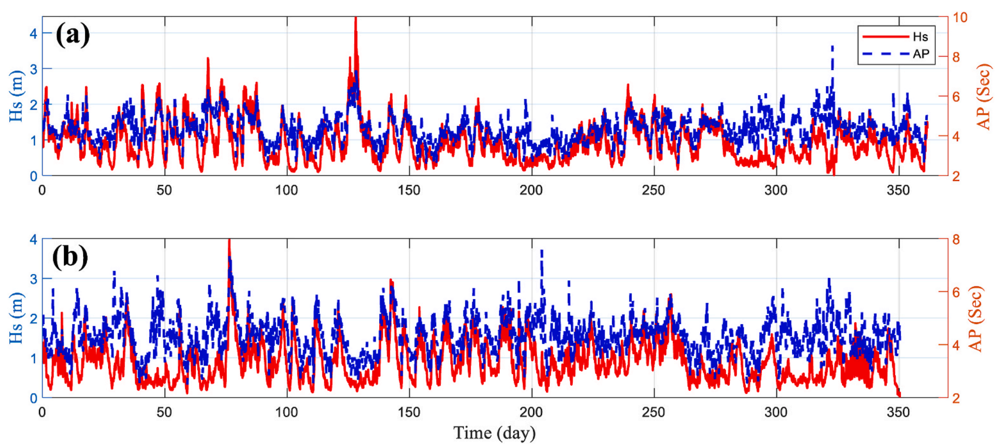

Fig. 5. Observed datasets of significant wave height (Hs) and hourly average wave period (AP) for (a) 2009 and (b) 2010.

where, o_i and y_i are observed and predicted Hs; n is the number of samples; $\bar{o}$, o_{max} and o_{min} are the mean, maximum, and minimum of observed Hs, respectively.

3. Study area and available datasets

The datasets of wave characteristics (Hs and AP) for the buoy located in Jeddah, Saudi Arabia, are used. The data are available on NOAA's website, station No. 23020, for two years (2009 and 2010) (NDBC - Station 23020 Recent Data (noaa.gov)). The buoy coordinate is 22.162° N 38.500° E, and the water depth is 694 m. Fig. 4 shows the location of the Jeddah buoy station. Some studies have been implemented in the study area for wave and wind prediction (Albarakati and Aboobacker, 2018; Fery et al., 2015; Langodan et al., 2014; Shanas et al., 2017; Zubier, 2020). The wave climatology of the Red Sea was proposed by Langodan et al. (2017). At the Jeddah station, the wave distribution manifests the dominant role of meteorological inputs from the Mediterranean Sea in the summer. North-east monsoon-connected southern winds in the winter leads to relatively high waves in the study area (Langodan et al., 2017). The best performance of Hs prediction for the study area is 0.81 in terms of R^2, with wave and wind characteristics (Zubier, 2020). The power spectra of waves have changed throughout the year; 58%, 28%, and 14% of waves are dominated by the unidirectional system, superimposed system, and both systems waves, respectively (Albarakati and Aboobacker, 2018; Shanas et al., 2017). It means that the correlation between Hs and AP is high in time and frequency domains. The Hs and AP were collected for 1-h intervals. Fig. 5 shows the available data. Table 2 presents the statistics of Hs and AP. The Pearson correlation coefficient between Hs and AP is calculated; it is 0.68 and 0.64 for the datasets of 2009 and 2010, respectively (as presented in Appendix A3). Moreover, the *t*-test of datasets was calculated, the null hypothesis from a population with mean value of datasets at 5% significant *t*-test was tested; the results showed the *t*-test = 0 for 2009 and 2010 datasets. This means the null hypothesis at the 5% significance level is accepted. From Fig. 5, Table 2, and correlation calculation, it can be shown that there is a high linear correlation between wave characteristics. Thus, the time lag (delayed) or timing error between the input and output variables should affect the performance of the designed models (Dixit et al., 2015). Here the timing error of the 2010 dataset is higher than that of the 2009 dataset. In this paper, first: the 2009 data

Table 2
Statistical evaluation of training and validation datasets.

Datasets	Data number	Variable	Minimum	Maximum	Average
2009 (Training and testing)	8678	Hs (m)	0.010	4.460	0.914
		AP (Sec)	2.580	8.540	4.326
2010 (Validation)	8408	Hs (m)	0.000	3.970	0.888
		AP (Sec)	2.490	7.580	4.333

Table 3
Trail-and error for designing diagram of RNN and NNARX models.

Hidden layers	Neurons No.	RNN		NNARX	
		R^2	Training time (min)	R^2	Training time (min)
1	10	0.981	0.06	0.979	0.000
	20	**0.982**	**0.32**	0.978	0.010
	30	0.983	4.51	0.980	0.010
2	[20 5]	0.982	0.38	**0.980**	**0.01**
	[20 10]	0.984	1.33	0.901	0.010
	[20 20]	0.984	11.48	0.980	0.030
3	[20 10 5]	0.982	1.37	0.978	0.020
	[10 10 10]	0.982	0.53	0.980	0.010
	[20 20 20]	0.986	36.05	0.968	0.100

are used to design the models. The first 80% of data were used into training phase and the remaining 20% were used into testing phase. The training and testing datasets are used to estimate the model parameters (see algorithm A1). Then, the whole 2009 and 2010 data are used to evaluate and validate the proposed models in predicting the time series of Hs (see Figure A1).

4. Results and discussion

To design the proposed model for Hs prediction based on Hs and AP, the appropriate number of hidden layers and neurons are performed. Models RNN[2,(k),1] and NNARX[2,(k),1], k columns refer to the number of hidden layers, and each column contains the number of neurons, are attempted. Table 3 presents some attempts with 50 epochs for designing RNN and NNARX models; the overall R^2 is presented. One delay is used in RNN, or a 1-h time head is used for designing the model's structures to decrease the timing error impact of input variables on predicting a 1-h time head. This assumption is used to design one structure for different time head cases in the time-series prediction of Hs. From Table 3, the accuracy variation of the RNN model with a different number of hidden layers is shown insignificant, as well as for the number of neurons. To decrease the time-consuming, we select one hidden layer with 20 neurons. Similarly, the best performance structure of NNARX is two layers with 20 and 5 neurons. Therefore, the best structure models are RNN [2,20,1], one hidden layer with 20 neurons, and NNARX [2,(20 5),1], two hidden layers; the first contains 20 neurons, and the second includes five neurons. After that the same structure was applied to predict other lead times. The RNNARX model is designed using the best structures of RNN and NNARX with a cascade of input (Fig. 2 and A1).

The design and validation of the proposed models are evaluated and compared in predicting Hs with hourly and daily time heads. Tables 4–6 present the performances of RNN, NNARX, and RNNARX models, respectively, at different time heads for the designing and validation stages. The overall model performances are presented in the designing stage using the whole 2009 dataset. Appendix A4 presents the training, testing and overall (designing) stages performances of RNNARX model at 6 h time lead. From Figure A3, it can be seen that the designing stage can be used to represent the overall performance of training and testing stages. Fig. 6 shows the performance of the three models at 6 h of lead times in the designing and validation stages. Fig. 7 shows the performance of the three models at 12 h of lead times.

Table 4
Statistical indices of RNN model performance in the design and validation stages.

	2009					2010				
Time (h)	R^2	RMSE (m)	MAE (m)	XAE (m)	PE (%)	R^2	RMSE (m)	MAE (m)	XAE (m)	PE (%)
1	**0.982**	**0.072**	**0.051**	**0.651**	**1.609**	0.799	0.283	0.213	1.012	7.125
3	0.944	0.124	0.092	1.055	2.790	**0.911**	**0.147**	**0.104**	**1.376**	**3.714**
6	0.858	0.188	0.149	1.868	4.235	0.778	0.216	0.169	1.572	5.430
12	0.735	0.240	0.205	2.019	5.384	0.539	0.287	0.251	2.096	7.219
24	0.484	0.271	0.287	2.133	6.098	0.262	0.335	0.324	3.183	8.444

Table 5
Statistical indices of NNARX model performance in the design and validation stages.

	2009					2010				
Time (h)	R^2	RMSE (m)	MAE (m)	XAE (m)	PE (%)	R^2	RMSE (m)	MAE (m)	XAE (m)	PE (%)
1	**0.980**	**0.076**	**0.054**	**0.672**	1.719	0.973	0.083	0.055	1.067	2.081
3	0.980	0.075	0.051	1.317	1.680	**0.974**	**0.082**	**0.053**	**1.601**	**2.057**
6	**0.983**	**0.071**	**0.050**	**0.749**	1.589	0.972	0.083	0.054	1.398	2.098
12	0.977	0.081	0.048	2.325	1.827	0.922	0.151	0.064	4.126	3.795
24	0.956	0.116	0.049	4.715	2.606	0.891	0.168	0.070	5.415	4.230
36	0.905	0.180	0.049	5.493	4.036	0.689	0.372	0.111	6.122	9.363

Table 6
Statistical indices of RNNARX model performance in the design and validation stages.

	2009					2010				
Time (h)	R^2	RMSE (m)	MAE (m)	XAE (m)	PE (%)	R^2	RMSE (m)	MAE (m)	XAE (m)	PE (%)
1	0.981	0.074	0.053	0.621	1.672	0.913	0.154	0.113	1.346	3.878
3	0.981	0.074	0.052	0.695	1.659	0.971	0.085	0.055	1.678	2.151
6	0.981	0.074	0.052	0.787	1.657	0.971	0.086	0.055	1.379	2.155
12	0.981	0.073	0.051	0.883	1.643	0.965	0.097	0.057	2.593	2.449
24	**0.982**	**0.072**	**0.051**	**1.091**	**1.629**	0.964	0.093	0.058	1.603	2.351
36	0.981	0.073	0.052	0.653	1.645	0.976	0.077	0.055	0.795	1.952
48	0.981	0.074	0.050	0.955	1.654	0.943	0.116	0.061	2.414	2.934
72	0.981	0.074	0.048	2.066	1.674	0.928	0.135	0.066	3.070	3.397
96	0.970	0.095	0.049	3.701	2.139	**0.905**	**0.149**	**0.080**	**2.953**	**3.745**
120	0.963	0.104	0.048	2.989	2.331	0.834	0.213	0.084	5.544	5.377

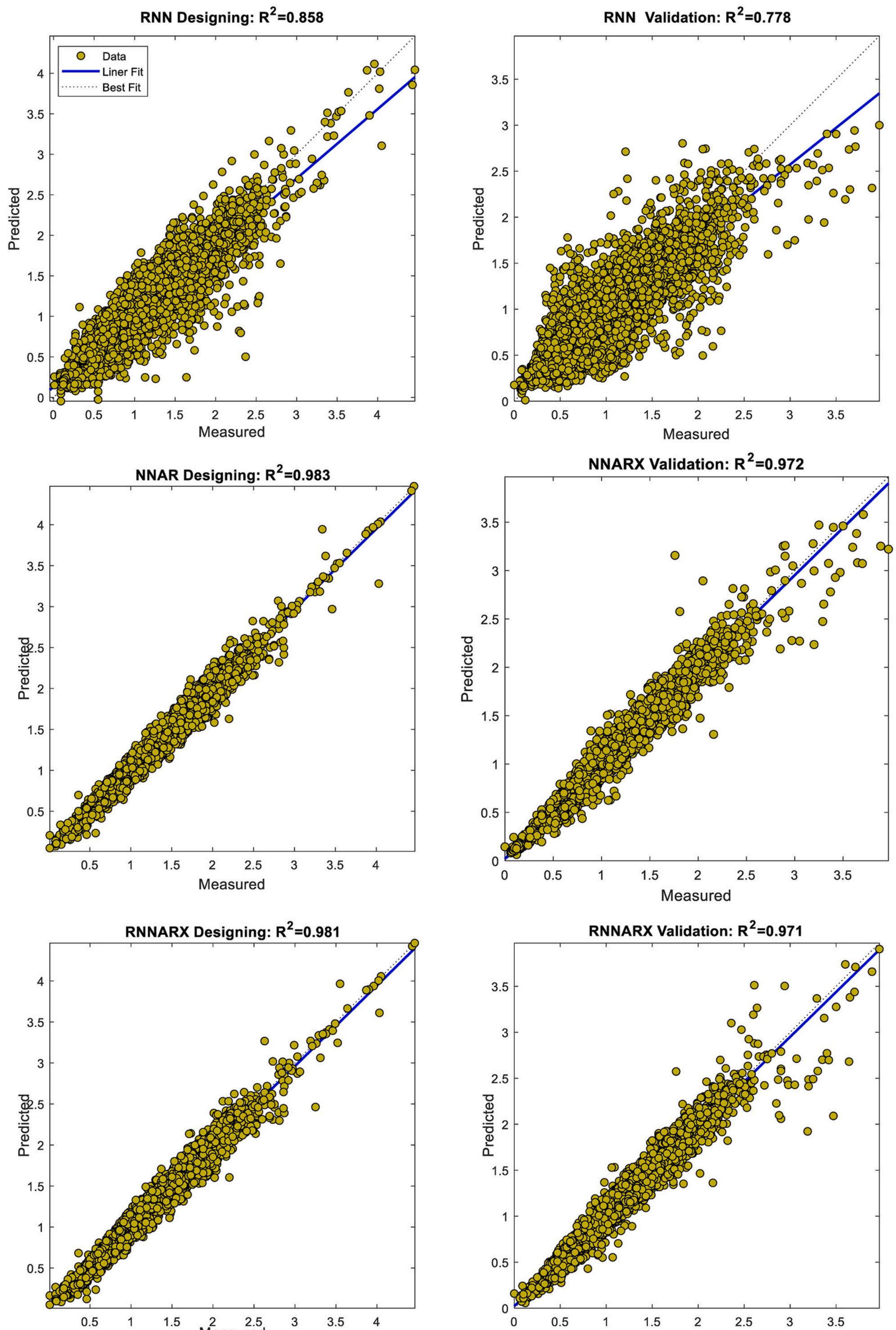

Fig. 6. Predicting 6 h, left is the designing, and right is the validation of the Red Sea significant wave height (Hs) for the recurrent neural network (RNN), NNAR, and RNNARX models. (For interpretation of the references to colour in this figure legend, the reader is referred to the Web version of this article.)

Table 4, Figs. 6 and 7 show that the RNN model performance in the designing stage is high up to 6 h of lead times. However, the RNN model performance in the validation stage is high up to 3 h of lead times. The percentage of model error is highly significant, reaching about 8.50% at forecasting 24 h of time head. Besides, the XAE of the model is 1.6, 2.1, and 3.2 m at 6, 12, and 24 h of lead times, respectively.

Table 5, Figs. 6 and 7 demonstrate that the performance of the NNARX model is highly significant for estimating the Hs values up to a one-day time head for the study area. The design stage shows that the performance of NNARX is high up to 36 h of lead times. The model error in the validation stage for the one-day time head is 4.23%. However, the XAE of the model approaches 4.13, 5.42, and 6.12 m for the predicting time head of 12, 24, and 36 h, respectively. It means that the model performance is suitable for sensing the Hs. However, with Hs of more than 2.5 m, its performance may decrease (Figs. 6 and 7). The comparison results of RNN and NNARX (Tables 4 and 5) indicate that the

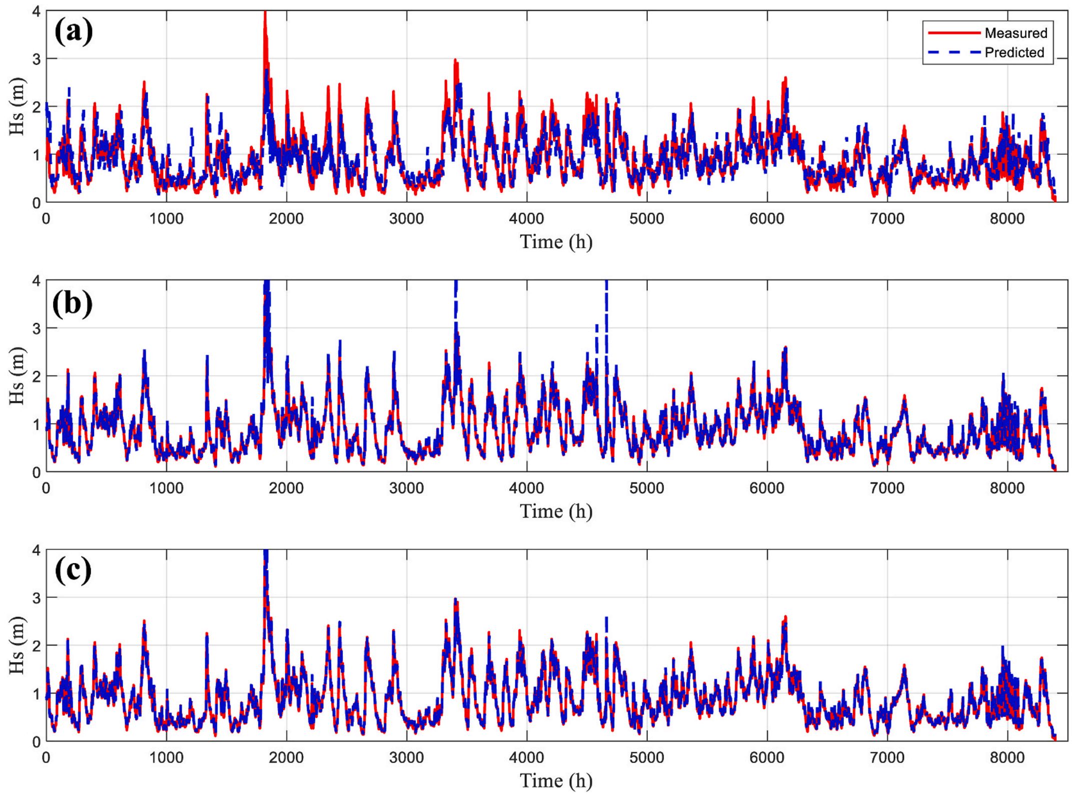

Fig. 7. (a) Recurrent neural network (RNN), (b) NARX neural network (NNARX), and (c) RNNARX models' performances at 12 h of lead time for the validation dataset.

NNARX method can predict the wave time-series more accurately in short and long-terms (up to one day lead time), and it is consistent with the results of Ardalani-Farsa and Zolfaghari (2010).

To improve the Hs prediction, NARX, RNN, and cascade neural networks were integrated into designing the developed model RNNARX. Table 6 presents the performance of RNNARX for Hs prediction up to 5 days' time head. Tables 4–6 show that the RNNARX outperforms other models in predicting Hs for short and long lead times; its performance is the best for predicting Hs up to 5-days' lead times in the designing and validation stages. The model error in the designing stage is 2.3% at 5 days' lead times. The percentage of model errors in the validation stage is 3.4%, 3.7%, and 5.4% for 3-, 4-, and 5-days lead times, respectively. Furthermore, the observed and predicted Hs are consistent up to 2.8 m. It is worth noting that in wave-wave modeling, the timing error affects the models' accuracy (Dixit et al., 2015). As shown in Tables 4–6, the time head affects the accuracy of the proposed models. In RNN, with an increase in time head, the accuracy of the model decreases in the designing stage. However, in the validation stage, because of the timing error between input and output variables, in the 1, 3, and 6 h of time head, the accuracy of RNN is acceptable. The accuracy in 3 h of time head is high due to the small effect of time error. In NNARX, the model overcomes the timing error in the designing and validation stages. The accuracy of the proposed model is high up to a one-day time head in the designing stage and up to 12 h in the validation stage. In RNNARX, the accuracy is improved in both designing and validation stages up to 5- and 4-days' time head, respectively. It means that the RNNARX model can be used to remove the prediction lag in the time-series prediction of Hs. Thus, integration and sequential learning of the neural network provide more acceptable results for Hs prediction at high lead times. The sequential system improved the performance of RNN and NNARX

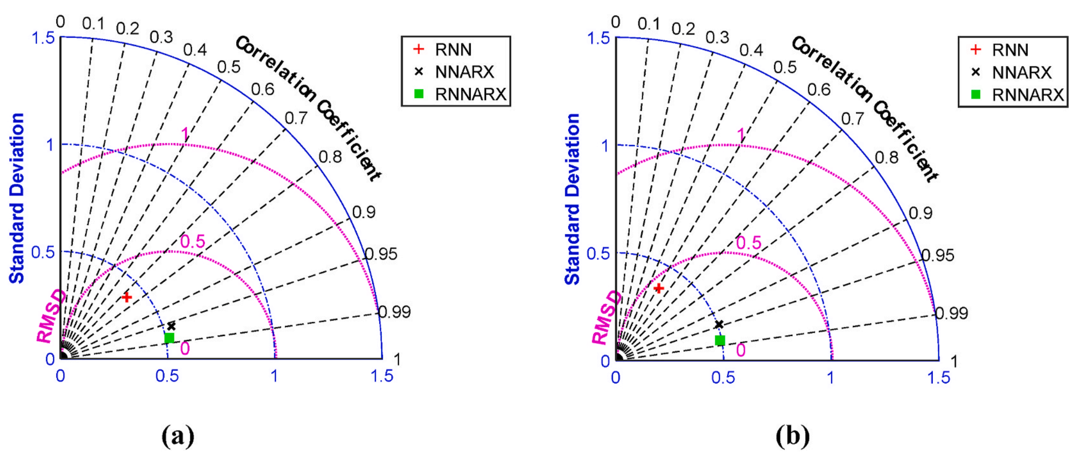

Fig. 8. Taylor diagram of the proposed models in the validation stage for (a) 12 h and (b) 24 h of lead times.

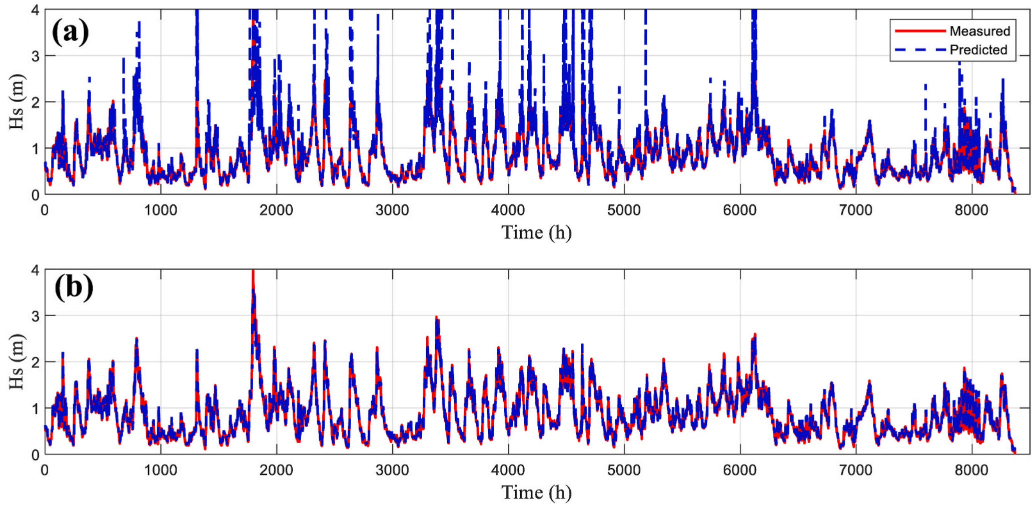

Fig. 9. (a) NARX neural network (NNARX) and (b) RNNARX models' performances at 36 h of lead time for the validation dataset.

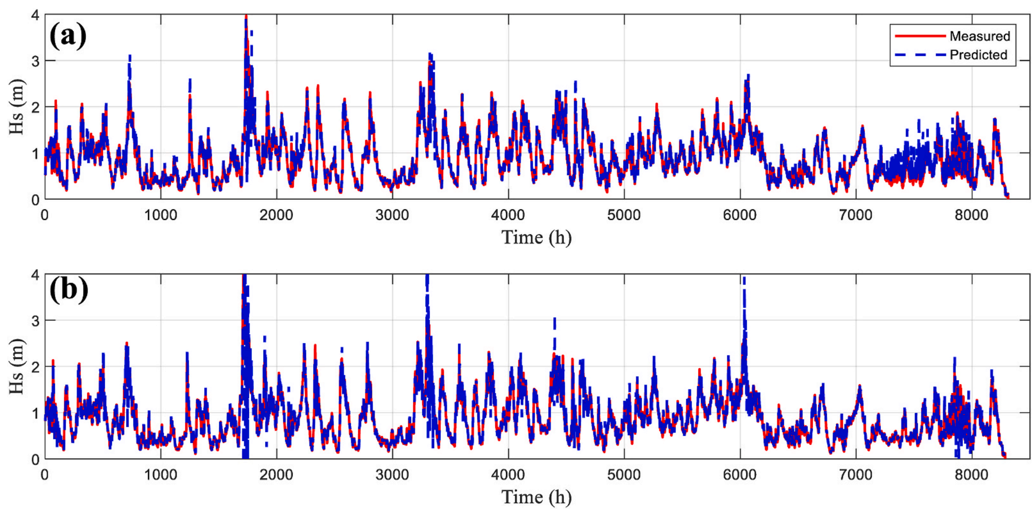

Fig. 10. RNNARX models performance for significant wave height (Hs) prediction at (a) 4 and (b) 5-days' time head.

models for the time-series prediction of Hs. The comparison results of RNN, NNARX, and RNNARX show that the performance of NNARX is better than RNNARX in terms of percentage of model errors up to 6 h of lead times for Hs prediction. For more than 6 h of lead times, the RNNARX achieves a high performance up to 5 days' lead times. Therefore, to decrease the complexity of calculation and time-consuming, the NNARX can be used to estimate the Hs in the Red Sea for the 6 h of lead times; for more than 6 h of time head, the RNNARX is better to use.

For more investigation, Fig. 8 shows the overall evaluation diagram, Taylor diagram, which is used to compare the models' performance in one chart. In a single plot, the Taylor diagram evaluates the degree of correspondence between the measured and predicted Hs in terms of Pearson correlation coefficients (black dashed contour), standard deviation (blue dashed contour), and RMS difference (RMSD) (purple dotted contour). The zero RMSD, lower standard deviation contour and high contour lines of correlation present the best solution for predicting values. It means that the model achieves the best performance in the correlation (high correlation), standard error (with small), and RMSD (small values). The models' performances are compared for predicting 12 h and 24 h of lead times. As shown in Fig. 8 and Tables 4–6, the RNNARX model achieves the performance for Hs prediction at 12 and 24 h of lead times. The RNNARX model performance is approximately equal for both lead times. It means that the RNNARX model is better for long-term time-series prediction of Hs.

Fig. 9 shows the performances of models NNARX and RNNARX for predicting 36 h of lead times. Fig. 10 shows the RNNARX model performance for predicting wave height at 4- and 5-day' time head. Tables 5 and 6 and Fig. 9 show the performance of the NNARX model, which is insignificant for predicting high lead times. The maximum error for the NNARX model is 6.12 m at 36 h of lead times. The performance of RNNARX is high with a XAE 0.80 m at the same time head. Furthermore, the percentages of the model's errors for Hs prediction are 9.4% and 1.95% for the NNARX and RNNARX models, respectively, at 36 h of lead times. The agreement between the observed and predicted Hs is low in the NNARX model for 36 h of lead times, while via versa is observed for the RNNARX model performance.

Additionally, the RNNARX model performance is high for predicting 5-days' time head. A high correlation (with 0.90 and 0.83) is observed for the model performance at 4- and 5-days' lead times, respectively. Furthermore, the percentage of model error is 2.95% and 5.54% for predicting 4- and 5-days' head times, respectively. These results indicate that the RNNARX can be used for long-term time-series prediction of Hs.

In summary, the results of the RNNARX model and previous soft-computing models (Table 1) (which mostly studied the prediction of Hs up to 12–36 h) confirm that the proposed model can be efficiently used for short and long-term prediction of Hs.

5. Conclusions

This study develops a new approach that can be used for long-period time-series prediction of Hs of Seas. The approach can deal with the long-period time delay of input variables. The current wave characteristics were used for predicting Hs at different lead times. The new technique was used for predicting Hs in the Red Sea in Jeddah, Saudi Arabia. The one-year dataset was used to design a model, and another year was used for validation. The proposed model is an integration neural network method. The NNARX, RNN, and cascade techniques are developed as a sequential system to design the new approach RNNARX. The results of the RNNARX model evaluation and comparison with conventional and previous studies results showed that the RNNARX outperforms RNN and NNARX in the prediction of Hs for high lead times. Additionally, the sequential system improved the performances of RNN and NNARX models for the time-series prediction of Hs. The performance of RNNARX is suitable for predicting 5-days' lead times. A high correlation (with 0.90 and 0.83) is observed for the model performance at 4- and 5-days' lead times, respectively. Furthermore, the percentage of the model error is 2.95% and 5.54% for predicting 4- and 5-days' head times, respectively. These results showed that the RNNARX model can accurately be used for long-term time-series prediction of Hs and can be implemented after calibration in similar areas.

CRediT author contribution statement

Yehia Miky: Investigation, Validation, Writing – review & editing, Funding acquisition. **Mosbeh R. Kaloop:** Conceptualization, Resources, Data curation, (data assessment), Investigation, Methodology, Software, Formal analysis, Validation, Writing – original draft, Writing – review & editing. **Mohamed T. Elnabwy:** Data curation, (data assessment), Investigation, Validation, Writing – review & editing. **Ahmad Baik:** Validation, review. **Ahmed Alshouny:** Investigation, Validation, review.

Declaration of competing interest

The authors declare that they have no known competing financial interests or personal relationships that could have appeared to influence the work reported in this paper.

Acknowledgement

This research work was funded by Institutional Fund Projects under grant No. (IFPHI-233-137-2020). Therefore, authors gratefully acknowledge technical and financial support from the Ministry of Education and King Abdulaziz University, DSR, Jeddah, Saudi Arabia.

Appendix A. Supplementary data

Supplementary data related to this article can be found at https://doi.org/10.1016/j.oceaneng.2021.109958.

References

Akhil, P., Deka, P., 2017. "Application of machine learning techniques in wave height forecasting in marine environment–A review. International Journal of Innovative Research in Science, Engineering and Technology 6 (5), 9649–9654. http://www.ijirset.com/upload/2017/may/300_Application.pdf.

Albarakati, A., Aboobacker, V.M., 2018. Wave transformation in the nearshore waters of Jeddah, west coast of Saudi Arabia. Ocean Eng. 163, 599–608. https://doi.org/10.1016/j.oceaneng.2018.06.041.

Ali, M., Prasad, R., Xiang, Y., Deo, R.C., 2020. Near real-time significant wave height forecasting with hybridized multiple linear regression algorithms. Renew. Sustain. Energy Rev. 132, 110003. https://doi.org/10.1016/j.rser.2020.110003.

Ardalani-Farsa, M., Zolfaghari, S., 2010. "Chaotic time series prediction with residual analysis method using hybrid elman–NARX neural networks. Neurocomputing 73 (13–15), 2540–2553. https://doi.org/10.1016/j.neucom.2010.06.004.

Ardhuin, F., Herbers, T.H.C., 2005. Numerical and physical diffusion: can wave prediction models resolve directional spread? J. Atmos. Ocean. Technol. 22 (7), 886–895. https://doi.org/10.1175/JTECH1723.1.

Bolderman, M., Lazar, M., Butler, H., 2021. Physics-Guided Neural Networks for Inversion-Based Feedforward Control Applied to Linear Motors arXiv 2021, arXiv:2103.060922021.

Blackmar, P.J., Cox, D.T., Wu, W.-C., 2014. Laboratory observations and numerical simulations of wave height attenuation in heterogeneous vegetation. J. Waterw. Port, Coast. Ocean Eng. 140 (1), 56–65. https://doi.org/10.1061/(ASCE)WW.1943-5460.0000215.

Canchala, T., Alfonso-Morales, W., Carvajal-Escobar, Y., Cerón, W.L., Caicedo-Bravo, E., 2020. Monthly rainfall anomalies forecasting for southwestern Colombia using artificial neural networks approaches. Water 12 (9), 2628. https://doi.org/10.3390/w12092628.

Chen, J., Chaudhari, N.S., 2004. Improvement of bidirectional recurrent neural network for learning long-term dependencies. Proceedings of the 17th International Conference on Pattern Recognition 4, 593–596. https://doi.org/10.1109/ICPR.2004.1333842, 2004. ICPR 2004., 2004.

Chen, X., Chen, Q., Zhan, J., Liu, D., 2016. Numerical simulations of wave propagation over a vegetated platform. Coast Eng. 110, 64–75. https://doi.org/10.1016/j.coastaleng.2016.01.003.

Deo, M.C., Naidu, C., 1998. Real time wave forecasting using neural networks. Ocean Eng. 26 (3), 191–203. https://doi.org/10.1016/S0029-8018(97)10025-7.

Dixit, P., Londhe, S., Dandawate, Y., 2015. Removing prediction lag in wave height forecasting using neuro-wavelet modeling technique. Ocean Eng. 93, 74–83. https://doi.org/10.1016/j.oceaneng.2014.10.009.

Duan, W., Huang, L., 2016. A hybrid EMD-AR model for nonlinear and non-stationary wave forecasting. J. Zhejiang Univ. - Sci. 17, 115–129. https://doi.org/10.1631/jzus.A1500164.

Elman, J.L., 1990. Finding structure in time. Cognit. Sci. 14 (2), 179–211. https://doi.org/10.1207/s15516709cog1402_1.

Emmanouil, S., Aguilar, S.G., Nane, G.F., Schouten, J.-J., 2020. Statistical models for improving significant wave height predictions in offshore operations. Ocean Eng. 206, 107249. https://doi.org/10.1016/j.oceaneng.2020.107249.

Etemad-Shahidi, A., Mahjoobi, J., 2009. "Comparison between M5′ model tree and neural networks for prediction of significant wave height in lake superior. Ocean Eng. 36 (15–16), 1175–1181. https://doi.org/10.1016/j.oceaneng.2009.08.008.

Fan, S., Xiao, N., Dong, S., 2020. A novel model to predict significant wave height based on long short-term memory network. Ocean Eng. 205, 107298. https://doi.org/10.1016/j.oceaneng.2020.107298.

Fery, N., Al-Subhi, A.M., Zubier, K.M., Bruss, G., 2015. Evaluation of the sea state near Jeddah based on recent observations and model results. Journal of Operational Oceanography 8 (1), 1–10. https://doi.org/10.1080/1755876X.2015.1014636.

Gavin, H.P., 2020. The Levenberg-Marquardt Algorithm for Nonlinear Least Squares Curve-Fitting Problems. Duke University, USA (access. https://people.duke.edu/~hpgavin/ce281/lm.pdf. (Accessed 20 September 2021).

Gers, F., 2001. Long Short-Term Memory in Recurrent Neural Networks", PhD Thesis. Hannover University, Germany.

Gopinath, D.I., Dwarakish, G., 2016. Real-time prediction of waves using neural networks trained by particle Swarm optimization. The International Journal of Ocean and Climate Systems 7 (2), 70–79. https://doi.org/10.1177/1759313116642896.

James, S.C., Zhang, Y., O'Donncha, F., 2018. A machine learning framework to forecast wave conditions. Coast Eng. 137, 1–10. http://arxiv.org/abs/1709.08725.

Kaloop, M.R., Beshr, A.A.A., Zarzoura, F., Ban, W.H., Hu, J.W., 2020a. "Predicting lake wave height based on regression classification and multi input–single output soft computing models. Arabian Journal of Geosciences 13 (14), 1–14. https://doi.org/10.1007/s12517-020-05498-1.

Kaloop, M.R., Kumar, D., Zarzoura, F., Roy, B., Hu, J.W., 2020b. A wavelet-particle Swarm optimization-extreme learning machine hybrid modeling for significant wave height prediction. Ocean Eng. 213 https://doi.org/10.1016/j.oceaneng.2020.107777.

Kanan, H.R., Faez, K., 2004. Wave height forecasting using cascade correlation neural network. In WSCG POSTERS proceedings 77–80. WSCG'2004, February 2-6, 2004, Plzen, Czech Republic.

Kolen, J.F., Kremer, S.C., 2001. Gradient FLow in Recurrent Nets: the Difficulty of Learning LongTerm Dependencies. In: A Field Guide to Dynamical Recurrent Networks. IEEE, pp. 237–243. https://doi.org/10.1109/9780470544037.ch14, 2001.

Kumar, N.K., Savitha, R., Mamun, A Al, 2017. Regional ocean wave height prediction using sequential learning neural networks. Ocean Eng. 129, 605–612. https://doi.org/10.1016/j.oceaneng.2016.10.033.

Kumar, N.K., Savitha, R., Mamun, A Al, 2018. Ocean wave height prediction using Ensemble of extreme learning machine. Neurocomputing 277, 12–20. https://doi.org/10.1016/j.neucom.2017.03.092.

Langodan, S., Cavaleri, L., Pomaro, A., Vishwanadhapalli, Y., Bertotti, L., Hoteit, I., 2017. "The climatology of the Red Sea–Part 2: the waves. Int. J. Climatol. 37 (13), 4518–4528. https://doi.org/10.1002/joc.5101.

Langodan, S., Cavaleri, L., Viswanadhapalli, Y., Hoteit, I., 2014. The Red Sea: a natural laboratory for wind and wave modeling. J. Phys. Oceanogr. 44 (12), 3139–3159. https://doi.org/10.1175/JPO-D-13-0242.1.

Le, X.H., Ho, H.V., Lee, G., Jung, S., 2019. Application of long short-term memory (LSTM) neural network for flood forecasting. Water 11 (7), 1387. https://doi.org/10.3390/w11071387.

Li, M., Liu, K., 2020. Probabilistic prediction of significant wave height using dynamic bayesian network and information Flow. Water 12 (8), 2075. https://doi.org/10.3390/w12082075.

Mafi, S., Amirinia, G., 2017. Forecasting hurricane wave height in gulf of Mexico using soft computing methods. Ocean Eng. 146, 352–362. https://doi.org/10.1016/j.oceaneng.2017.10.003.

Mahjoobi, J., Mosabbeb, E., 2009. Prediction of significant wave height using regressive support vector machines. Ocean Eng. 36 (5), 339–347. https://doi.org/10.1016/j.oceaneng.2009.01.001.

Mandal, S., Prabaharan, N., 2006. Ocean wave forecasting using recurrent neural networks. Ocean Eng. 33 (10), 1401–1410. https://doi.org/10.1016/j.oceaneng.2005.08.007.

Mathworks, 2016. MATLAB Mathworks-MATLAB & Simulink. www.mathworks.com. //doi.org/2016-11-26, 2016.

Paplińska-Swerpel, B., Paszke, Ł., 2006. Application of neural networks to the prediction of significant wave height at selected locations on the baltic sea. Arch. Hydroeng. Environ. Mech. 53 (3), 83–201. Availble online (Access on June 19, 2021). http://www.ibwpan.gda.pl/storage/app/media/ahem/ahem53str183.pdf.

Peres, D.J., Iuppa, C., Cavallaro, L., Cancelliere, A., Foti, E., 2015. Significant wave height record extension by neural networks and reanalysis wind data. Ocean Model. 94, 128–140. https://doi.org/10.1016/j.ocemod.2015.08.002.

Pirhooshyaran, M., Snyder, L.V., 2020. Forecasting, hindcasting and feature selection of ocean waves via recurrent and sequence-to-sequence networks. Ocean Eng. 207, 107424. https://doi.org/10.1016/j.oceaneng.2020.107424.

Prahlada, R., Deka, P.C., 2015. Forecasting of time series significant wave height using wavelet decomposed neural network. Aquatic Procedia 4, 540–547. https://doi.org/10.1016/j.aqpro.2015.02.070.

Roy, C., Motamedi, S., Hashim, R., Shamshirband, S., Petković, D., 2016. A comparative study for estimation of wave height using traditional and hybrid soft-computing methods. Environmental Earth Sciences 75 (7), 590. https://doi.org/10.1007/s12665-015-5221-x.

Sadeghifar, T., Motlagh, N.M., Azad, T.M., Mahdizadeh, M.M., 2017. Coastal wave height prediction using recurrent neural networks (RNNs) in the south caspian sea. Mar. Geodes. 40 (6), 454–465. https://doi.org/10.1080/01490419.2017.1359220.

Schmidhuber, J., 1992. Learning complex, extended sequences using the principle of history compression. Neural Comput. 4 (2), 234–242. https://doi.org/10.1162/neco.1992.4.2.234.

Shamshirband, S., Mosavi, A., Rabczuk, T., Nabipour, N., Chau, K., 2020. Prediction of significant wave height; comparison between nested grid numerical model, and machine learning models of artificial neural networks, extreme learning and support vector machines. Engineering Applications of Computational Fluid Mechanics 14 (1), 805–817. https://doi.org/10.1080/19942060.2020.1773932.

Shanas, P.R., Aboobacker, V.M., Alaa, M.A.A., Khalid, M.Z., 2017. Superimposed wind-waves in the Red Sea. Ocean Eng. 138, 9–22. https://doi.org/10.1016/j.oceaneng.2017.04.020.

Ti, Z., Zhang, M., Wu, L., Qin, S., Wei, K., Li, Y., 2018. Estimation of the significant wave height in the nearshore using prediction equations based on the response surface method. Ocean Eng. 153, 143–153. https://doi.org/10.1016/j.oceaneng.2018.01.081.

Tian, Y., Xu, Y.-P., Yang, Z., Wang, G., Zhu, Q., 2018. Integration of a parsimonious hydrological model with recurrent neural networks for improved streamflow forecasting. Water 10 (11), 1655. https://doi.org/10.3390/w10111655.

Tom, T., Ikemoto, A., Mase, H., Kawasaki, K., Takeda, M., Kim, S., 2019. Wave prediction in the sea of Japan by deep learning using meteorological data. Journal of Japan Society of Civil Engineers, Ser. B2 (Coastal Engineering) 75 (2), I_145–I_150. https://doi.org/10.2208/kaigan.75.I_145.

Vimala, J., Latha, G., Venkatesan, R., 2012. Application of soft computing tools for wave prediction at specific locations in the arabian sea using moored buoy observations. International Journal of Ocean and Climate Systems 3 (4), 255–264. https://doi.org/10.1260/1759-3131.3.4.255.

Warsito, B., Santoso, R., Suparti, Yasin, H., 2018. Cascade forward neural network for time series prediction. J. Phys. Conf. 1025, 012097 https://doi.org/10.1088/1742-6596/101/25/012097.

WMO, 1998. Guide to Wave Analysis and Forecasting. WMO-No, p. 702.

Xie, H., Tang, H., Liao, Y., 2009. Time series prediction based on NARX neural networks: an advanced approach. In: In 2009 International Conference on Machine Learning and Cybernetics, vols. 1275–79. IEEE. https://doi.org/10.1109/ICMLC.2009.5212326.

Yetkin, M., Kim, M.S., Kim, Y., 2017. Mooring line top-tension prediction using NARX. In: In Proceedings of the International Offshore and Polar Engineering Conference, pp. 196–202.

Yetkin, M., Kim, Y., 2019. Time series prediction of mooring line top tension by the NARX and volterra model. Appl. Ocean Res. 88, 170–186. https://doi.org/10.1016/j.apor.2019.04.013.

Yuen, Y.H., Lazar, M., Butler, H., 2019. DatA–Driven Neural Feedforward Controller Design for Industrial Linear Motors. In: 2019 23rd International Conference on System Theory, Control and Computing. ICSTCC, pp. 461–467. https://doi.org/10.1109/ICSTCC.2019.8885434, 2019.

Zubier, K.M., 2020. Using an artificial neural network for wave height forecasting in the Red Sea. Indian Journal of Geo-Marine Sciences 49 (2), 184-19. http://nopr.niscair.res.in/handle/123456789/54084.

Zubier, K.M., Eyouni, L.S., 2020. Investigating the role of atmospheric variables on sea level variations in the eastern central Red Sea using an artificial neural network approach. Oceanologia 62 (3), 267–290. https://doi.org/10.1016/j.oceano.2020.02.002.